Fuel Efficient Connected Cruise Control for Heavy Duty Vehicles

C. R. He & G. Orosz
Department of Mechanical Engineering
University of Michigan, Ann Arbor, MI 48109, USA
E-mail: hchaozhe@umich.edu
J. I. Ge
Department of Computational and Mathematical Sciences
California Institute of Technology, Pasadena, CA 91125, USA

Topics/Vehicle Automation and Connection

July 19, 2018

In this paper, we present a data-based approach that can be used to improve the fuel economy of connected automated vehicles. We propose a connected cruise control algorithm that utilizes beyond-line-of-sight information while responding to the motion of multiple vehicles ahead. We demonstrate that by optimizing the control parameters one can achieve significant fuel economy improvements for a class-8 truck. The results are validated using a high-fidelity TruckSim model.

1 INTRODUCTION

Improving fuel efficiency for ground vehicles, in particular for heavy duty vehicles, carries both economical and societal benefits. Vehicle automation and wireless vehicle-to-everything (V2X) communication may be used to achieve this. Using geo-location and grade information to optimize speed profile was shown to improve fuel economy in sparse traffic conditions [1]. In heavy traffic, numerical optimization methods can be used to achieve better fuel economy when the motion of the vehicle immediately ahead can be accurately predicted [2]. However, when the preceding vehicle is driven by a human driver such prediction may become inaccurate.

On the other hand, wireless vehicle-to-vehicle (V2V) communication may be used to monitor the motion of multiple vehicles ahead even when they are beyond the line of sight. Using such information in the longitudinal controller of a connected automated vehicle, referred to as connected cruise control [3–6], may lead to significant energy savings. In this paper, we utilize traffic data collected from a chain of human-driven vehicles and design connected cruise controllers to improve fuel economy for a class-8 truck inserted into the traffic flow. We establish an optimization method that allows energy-efficient responses to traffic perturbations and we demonstrate its impacts on fuel economy using high-fidelity TruckSim simulations.

2 DATA ANALYSIS, MODELING, AND CONTROL DESIGN

In this section, we discuss how real-time traffic data can be utilized to control a connected automated truck. We consider a driving scenario where the truck drives behind several human-driven vehicles on a segment of flat road; see Fig. 1(a). All vehicles are equipped with GPS and V2X devices so they can broadcast their positions and velocities. The truck utilizes this information in order to control its longitudinal motion through a connected cruise control algorithm.

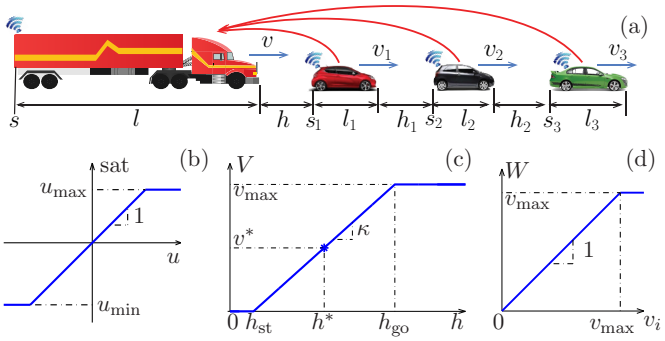

Figure 1: (a) Layout of the connected vehicle system consisting of three human-driven vehicles and a heavy duty vehicle that is driven by a connected cruise control algorithm. (b) The saturation function in (2). (c) The range policy function (7). (d) The saturation function (8).

2.1 Traffic data

Velocity data of human-driven vehicles are displayed in Fig. 2(a.1-a.3) in three different driving scenarios. The green, black, and red curves correspond to the speed of vehicle 3, vehicle 2 and vehicle 1, respectively. Fig. 2(a.1) shows a scenario where the cars are driving around 30 [m/s] with very little speed variations. In Fig. 2(a.2) the speeds vary between 0 and 30 [m/s] such that the plateaus are connected by short periods of mild accelerations and decelerations. Finally, the speed profiles in Fig. 2(a.3) consist of constant speed driving around 25 [m/s] that is interrupted by short periods of braking and acceleration.

The differences between the different speed profiles are further emphasized through the Fourier components shown in Fig. 2(b.1-b.3,c.1-c.3). These can be used to reconstruct the speed profiles according to

$$\begin{aligned} v_i(t) &= v^* + \tilde{v}_i(t) \\ &= v^* + \sum_{j=1}^{m} \rho_{i,j} \sin(\omega_j t + \phi_{i,j}), \end{aligned} \tag{1}$$

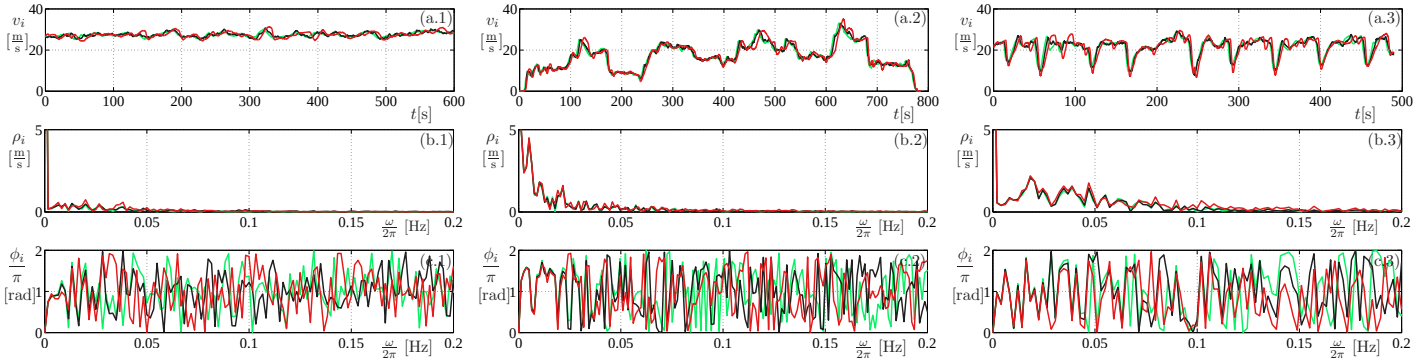

Figure 2: (a.1-a.3) Speed profiles of human-driven vehicles as function of time. (b.1-b.3) Amplitudes of the Fourier spectra as function of frequency. (c.1-c.3) Phases of the Fourier spectra as function of frequency; cf. (1).

along the time interval $t \in [0, T]$ where the time horizon T may be different for different traffic scenarios. Here we discretized frequency $\omega_j = j\Delta\omega$ with $\Delta\omega = 2\pi/T$ and used the notation $\rho_{i,j} = \rho_i(\omega_j)$ and $\phi_{i,j} = \phi_i(\omega_j)$ for the amplitude and phase angle at frequency ω_j. The constant Fourier component v^* is separated as this is the same for all vehicles in the chain.

Below we will utilize the Fourier decomposition (1) and select the control parameters in the connected cruise controller in order to optimize the energy efficiency of the truck. We will demonstrate that the three different profiles shown in Fig. 2 will lead to different sets of optimal parameters allowing us to "tailor" the connected cruise controllers to the traffic data.

2.2 Longitudinal dynamics

The longitudinal motion of the truck can be described by the simplified model

$$\begin{aligned} \dot{s}(t) &= v(t)\,, \\ \dot{v}(t) &= -f\big(v(t)\big) + \mathrm{sat}\big(u(t-\zeta)\big)\,, \end{aligned} \tag{2}$$

where the dots denote differentiation with respect to time t, s denotes the position of the rear bumper of the truck, v denotes its velocity; see Fig. 1(a).

The air resistance and rolling resistance are included in

$$f(v) = \frac{1}{m_{\mathrm{eff}}}(\gamma m \mathrm{g} + k v^2)\,, \tag{3}$$

where g is the gravitational constant, γ is the rolling resistance coefficient, k is the air drag constant, and the effective mass $m_{\mathrm{eff}} = m + I/R^2$ includes the mass of the vehicle m, the moment of inertia I of the rotating elements, and the wheel radius R [7]. The values of these parameters are listed in Table 1.

The commanded acceleration u is implemented by the engine and the brakes. The parameter ζ represents the actuator delay while the saturation function $\mathrm{sat}(\cdot)$ corresponds to the torque limits of these actuators; see Fig. 1(b). While the minimum $u_{\min}$ is independent of the speed, for the maximum we have $u_{\max} = \min\{\bar{u}_{\max}, P_{\max}/(m_{\mathrm{eff}} v)\}$ where $P_{\max}$ represents the power limit of the engine; see Table 1. In this paper we use the controller

$$u = a_{\mathrm{d}} + \tilde{f}(v)\,, \tag{4}$$

where a_{d} represent the acceleration demanded by the connected cruise controller (see below) while the term $\tilde{f}(v)$ is added to compensate for the air drag and the rolling resistance.

2.3 Connected cruise control design

Considering the scenario when the connected automated truck receives motion information about n human driven vehicles ahead, we propose the connected cruise controller

$$\begin{aligned} a_{\mathrm{d}}(t) = \alpha\Big(V\big(h(t-\xi_1)\big) - v(t-\xi_1)\Big) \\ + \sum_{i=1}^{n} \beta_i \Big(W\big(v_i(t-\xi_i)\big) - v(t-\xi_i)\Big)\,. \end{aligned} \tag{5}$$

where the headway

$$h = s_1 - s - l\,, \tag{6}$$

is the distance gap between the truck and the vehicle immediately ahead and l denotes the length of the truck. Moreover, α and β_i are the feedback gains while ξ_i represents the communication delay from vehicle i.

The range policy function

$$V(h) = \begin{cases} 0 & \text{if} \quad h \le h_{\mathrm{st}}\,, \\ \kappa(h - h_{\mathrm{st}}) & \text{if} \quad h_{\mathrm{st}} < h < h_{\mathrm{go}}\,, \\ v_{\max} & \text{if} \quad h \ge h_{\mathrm{go}}\,, \end{cases} \tag{7}$$

describes the desired velocity of the truck as a function of its headway; see Fig. 1(c). For a small headway ($h < h_{\mathrm{st}}$), the truck intends to stop; for a large headway ($h > h_{\mathrm{go}}$), it intends to travel with the speed limit $v_{\max}$; between h_{st} and h_{go} the desired velocity increases linearly, with the gradient $\kappa = v_{\max}/(h_{\mathrm{go}} - h_{\mathrm{st}})$. Finally, the saturation function

$$W(v_i) = \begin{cases} v_i & \text{if} \quad v_i \le v_{\max}\,, \\ v_{\max} & \text{if} \quad v_i > v_{\max}\,, \end{cases} \tag{8}$$

shown in Fig. 1(d) is included to stay below the speed limit when a preceding vehicle is speeding. In this paper, we use $v_{\max} = 30\,[\mathrm{m/s}]$, $h_{\mathrm{st}} = 5\,[\mathrm{m}]$ and $\kappa = 0.6\,[1/\mathrm{s}]$.

Parameter	Value
Mass (m)	29484 [kg]
Tire rolling resistance coefficient (γ)	0.006
Air drag coefficient (k)	3.84 [kg/m]
Tire rolling radius (R)	0.504 [m]
Rotational inertia (I)	39.9 [kg·m^2]
Gravitational constant (g)	9.81 [m/s^2]
Braking limit ($u_{\min}$)	-4 [m/s^2]
Acceleration limit ($\bar{u}_{\max}$)	1 [m/s^2]
Maximum engine power ($P_{\max}$)	300.65 [kW]

Table 1: Data of a 2012 Navistar Prostar truck [8].

3 ENERGY-OPTIMAL CONNECTED CRUISE CONTROL

In order to evaluate the influence of different traffic perturbations on energy efficiency, we define the cumulative energy consumption per unit mass as

$$w(t) = \int_0^t v(\tau) g\Big(\dot{v}(\tau) + f\big(v(\tau)\big)\Big)\,\mathrm{d}\tau\,, \tag{9}$$

where $t \in [0, T]$ and $g(x) = \max(0, x)$. For vehicles with internal combustion engines, fuel consumption typically increases with the energy consumption $w(t)$. However, as $w(t)$ is defined by the vehicle's motion, it can also be used to evaluate the energy consumption of electric or hybrid vehicles due to speed variations using an appropriate g function. Our goal here is to find the feedback gains β_i in (5) that minimize the (9).

3.1 Plant stability

Before searching for the energy-optimal feedback gains, it is necessary to obtain the stability boundaries to ensure that the connected automated truck is able to maintain constant speed when the vehicles ahead are traveling at constant speed. Thus, we consider the steady-state

$$v(t) \equiv v_i(t) \equiv v^* \,, \tag{10}$$

for $i = 1, \dots, n$ and

$$h(t) \equiv h^* \,, \quad v^* = V(h^*) \,, \tag{11}$$

cf. (7) and Fig. 1(c).

We define $\tilde{s}$, $\tilde{s}_1$, $\tilde{v}_i$, $i = 1, \dots, n$ as the perturbations about the equilibrium positions and velocities (cf. (1)) and assume that the influence of the physical effects $f(v)$ can be negated by $\tilde{f}(v)$. Then linearizing the dynamics (2,4,5) of the connected automated truck about (10), we obtain

$$\begin{aligned} \dot{\tilde{s}}(t) &= \tilde{v}, \\ \dot{\tilde{v}}(t) &= \alpha\Big(\kappa\big(\tilde{h}(t-\sigma_1)\big) - \tilde{v}(t-\sigma_1)\Big) \\ &\quad + \sum_{i=1}^{n} \beta_i \Big(\tilde{v}_i(t-\sigma_i) - \tilde{v}(t-\sigma_i)\Big) \,, \end{aligned} \tag{12}$$

where $\tilde{h} = \tilde{s}_1 - \tilde{s}$ is the perturbation about the equilibrium headway h^* and $\sigma_i = \xi_i + \zeta$ gives the total delay in the control loop. For simplicity, we consider $\sigma_i = \sigma$ for $i = 1, \dots, n$.

In order for the connected automated truck to be able to maintain its speed around the equilibrium, we require the linearized dynamics (12) to be plant stable [4]. That is, all roots of the characteristic equation

$$D(\lambda) = \lambda^2 \mathrm{e}^{\sigma\lambda} + \left(\alpha + \sum_{i=1}^{n} \beta_i\right)\lambda + \alpha\kappa = 0 \,, \tag{13}$$

must be located in the left half complex plane. Thus, the design parameters α and β_i need to be selected from the domain enclosed by

$$\alpha = 0 \,, \tag{14}$$

and

$$\begin{aligned} \alpha &= \frac{\Omega^2}{\kappa}\cos(\Omega\sigma) \,, \\ \sum_{i=1}^{n} \beta_i &= \Omega \sin(\Omega\sigma) - \frac{\Omega^2}{\kappa}\cos(\Omega\sigma) \,, \end{aligned} \tag{15}$$

for $\Omega > 0$.

In Fig. 3, we plot the plant-stable domain in the $(\sum_{i=1}^{n} \beta_i, \alpha)$-plane for $\kappa = 0.6$ [1/s] and $\sigma = 0.7$ [s]. The black line highlights the plant-stable range of $\sum_{i=1}^{n} \beta_i$ for the headway feedback gain $\alpha = 0.4$ [1/s] that is chosen here based on safety considerations.

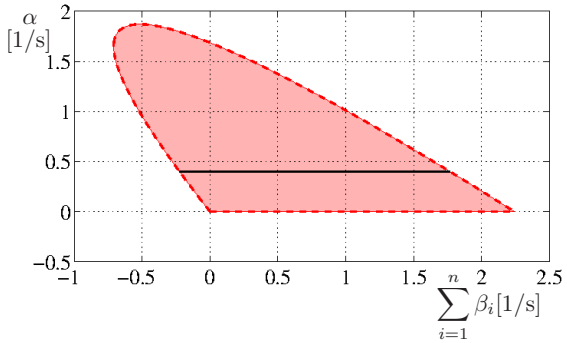

Figure 3: Stability diagram for $\kappa = 0.6$ [1/s] and $\sigma = 0.7$ [s] where the shaded region corresponds to plant stable parameters. The black line segment corresponds to $\alpha = 0.4$ [1/s].

3.2 Data-driven energy minimization

Since directly minimizing the energy consumption (9) may lead to designs that are overly sensitive here we propose an energy-optimal connected cruise control design by exploiting the Fourier decomposition of traffic perturbations.

Based on the linearized dynamics (12), the speed oscillation of the connected automated truck can be written as

$$\tilde{V}(\lambda) = \sum_{i=1}^{n} \Gamma_i(\lambda; \mathbf{p}_n)\tilde{V}_i(\lambda) \,, \tag{16}$$

where $\tilde{V}_i(\lambda)$ is the Laplace transform of the velocity perturbation $\tilde{v}_i(t)$. The vector $\mathbf{p}_n = [\alpha, \kappa, \beta_1, \dots, \beta_n]$ contains the design parameters, and the so-called link transfer function from the i-th vehicle to the connected automated truck can be formulated as

$$\begin{aligned} \Gamma_1(\lambda; \mathbf{p}_n) &= \frac{\alpha\kappa + \lambda\beta_1}{\lambda^2 \mathrm{e}^{\sigma\lambda} + \left(\alpha + \sum_{k=1}^{n} \beta_k\right)\lambda + \alpha\kappa} \,, \\ \Gamma_i(\lambda; \mathbf{p}_n) &= \frac{\lambda\beta_i}{\lambda^2 \mathrm{e}^{\sigma\lambda} + \left(\alpha + \sum_{k=1}^{n} \beta_k\right)\lambda + \alpha\kappa} \,, \end{aligned} \tag{17}$$

for $i = 2, \dots, n$.

Based on (1,16,17), the steady-state oscillation of the connected automated truck is given by

$$\begin{aligned} v(t) &= v^* + \tilde{v}(t) \\ &= v^* + \sum_{j=1}^{m} \sum_{i=1}^{n} \tilde{\rho}_{i,j}(\mathbf{p}_n) \sin\big(\omega_j t + \tilde{\phi}_{i,j}(\mathbf{p}_n)\big), \end{aligned} \tag{18}$$

where

$$\begin{aligned} \tilde{\rho}_{i,j}(\mathbf{p}_n) &= \rho_{i,j} \cdot \Gamma_i(\mathrm{i}\omega_j; \mathbf{p}_n) \,, \\ \tilde{\phi}_{i,j}(\mathbf{p}_n) &= \phi_{i,j} + \angle\, \Gamma_i(\mathrm{i}\omega_j; \mathbf{p}_n) \,. \end{aligned} \tag{19}$$

This can be rewritten as

$$\begin{aligned} v(t) &= v^* + \tilde{v}(t) \\ &= v^* + \sum_{j=1}^{m} D_j(\mathbf{p}_n) \sin\big(\omega_j t + \theta_j(\mathbf{p}_n)\big) \,, \end{aligned} \tag{20}$$

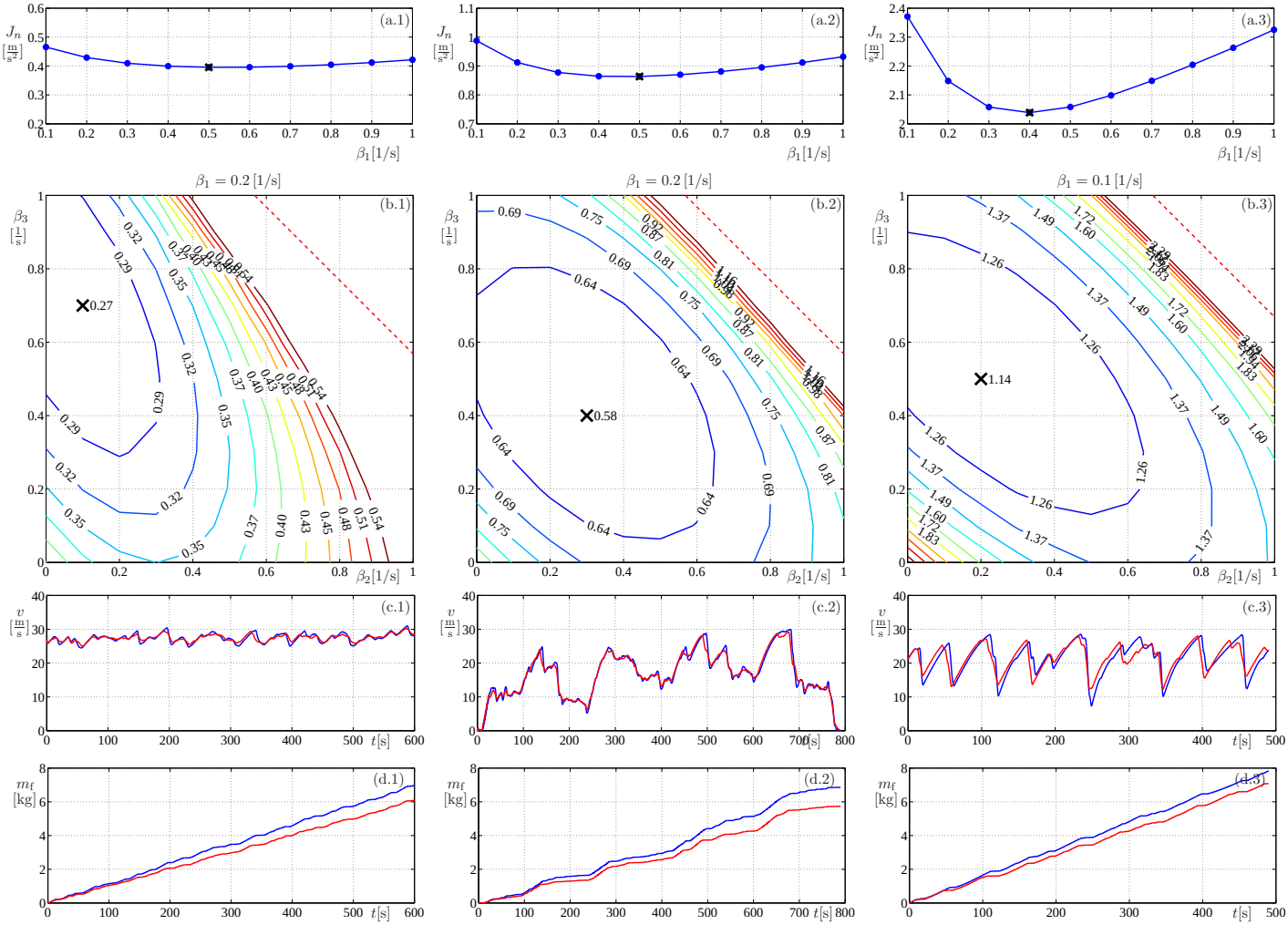

Figure 4: (a.1-a.3) The value of the cost (20) as function of the gain parameter β_1 when the truck only utilizes motion information from the vehicle immediately ahead. (b.1-b.3) The level sets of the cost (20) in the (β_2, β_3)-plane when the truck utilizes information from three vehicles ahead. (c.1-c.3) The speed profiles for the energy-optimal connected automated truck obtained by Trcuksim. Blue curves correspond to the cases when motion information from one car is utilized while red curves correspond the cases when motion information from all three vehicles are used. (d.1-d.3) The corresponding fuel consumption profiles.

where

$$D_j = \sqrt{\left(\sum_{i=1}^{n} \tilde{\rho}_{i,j} \cos \tilde{\phi}_{i,j}\right)^2 + \left(\sum_{i=1}^{n} \tilde{\rho}_{i,j} \sin \tilde{\phi}_{i,j}\right)^2},$$

$$\tan \theta_j = \frac{\sum_{i=1}^{n} \tilde{\rho}_{i,j} \sin \tilde{\phi}_{i,j}}{\sum_{i=1}^{n} \tilde{\rho}_{i,j} \cos \tilde{\phi}_{i,j}}. \tag{21}$$

We propose the minimization of the cost function

$$\min_{\mathbf{p}_n \in \mathbf{P}} J_n(\mathbf{p}_n) = \sqrt{\sum_{j=1}^{m} \omega_j^2 D_j^2(\mathbf{p}_n)}, \tag{22}$$

where $\mathbf{P}$ is the admissible set of $\mathbf{p}_n$ that ensures plant stability; see (14,15) and Fig. 3. Other specifications such as string stability may also be incorporated [9]. The details about the construction of (22) are provided in Appendix A. By computing the level sets of (22), the parameters in $\mathbf{p}_n$ can be related to the energy efficiency of the connected automated truck at the linear level. We remark that the computational demand of such minimization is very low.

The results of are summarized in Fig. 4 where the columns correspond those in Fig. 2. In order to create a benchmark, in panels (a.1-a.3) we show the values of J_n given in (22) when varying the control gain β_1 (with resolution 0.1 [1/s]) and $\beta_2 = \beta_3 = 0$. This means that the truck only utilizes motion information from its immediate predecessor. For the different speed profiles the values of J_n change significantly but the minimum is located around $\beta_1 = 0.4 - 0.5$ [1/s] as indicated by the black crosses. Then, in panels (b.1-b.3), we vary $\beta_1, \beta_2, \beta_3$ (again using resolution 0.1 [1/s]) to find the minima of J_n that are indicated by black crosses. The red dashed curves are the plant stability boundaries; cf. Fig. 3.

When comparing the minimum values of J_n in panels (a.k) and (b.k) in the k-th column, one may notice significant improvements. Even the minimum values along the lines $\beta_2 = 0$ and $\beta_3 = 0$ are significantly lower than for the case $\beta_2 = \beta_3 = 0$. This implies that utilizing motion information from more than one vehicle ahead can improve the energy efficiency of the truck. Also notice that the locations minima changes significantly when comparing the different columns. This shows that by selecting the gain combinations appropriately one may "tailor" the controller to the traffic scenario ahead to maximize the energy savings.

In order to demonstrate the impact of these energy savings on fuel economy we utilized a high fidelity model in Trucksim and we implemented the controller (4, 5). The corresponding velocity profiles are displayed in Fig. 4(c.1-c.3) where the blue curves correspond to the energy-optimal CCC when the truck only uses motion information from the vehicle immediately ahead while the red curves correspond to the energy-optimal CCC when motion information from all three vehicles ahead are utilized.

When comparing the blue and red curves the differences are not very significant though the red curves look smoother. The benefits become evident when looking at the fuel consumption in Fig. 4(d.1-d.3). This show that monitoring three vehicles ahead can lead to 10-15% fuel economy improvements compared to the case when only one vehicle ahead is monitored.

4 CONCLUSIONS

In this paper, we proposed a data-based method to improve the energy efficiency of connected automated trucks. We used an optimization method to design an energy efficient connected cruise controller based on the traffic data collected during road experiments. Using high-fidelity simulations in TruckSim, we demonstrated the fuel-economy benefits compared to a benchmark design.

REFERENCES

[1] V. Turri, B. Besselink, and K. H. Johansson, "Cooperative look-ahead control for fuel-efficient and safe heavy-duty vehicle platooning," *IEEE Transactions on Control Systems Technology*, vol. 25, no. 1, pp. 12–28, 2017.

[2] S. E. Li, Q. Guo, S. Xu, J. Duan, S. Li, C. Li, and K. Su, "Performance enhanced predictive control for adaptive cruise control system considering road elevation information," *IEEE Transactions on Intelligent Vehicles*, vol. 2, no. 3, pp. 150–160, 2017.

[3] J. I. Ge and G. Orosz, "Dynamics of connected vehicle systems with delayed acceleration feedback," *Transportation Research Part C*, vol. 46, pp. 46–64, 2014.

[4] G. Orosz, "Connected cruise control: modelling, delay effects, and nonlinear behaviour," *Vehicle System Dynamics*, vol. 54, no. 8, pp. 1147–1176, 2016.

[5] L. Zhang and G. Orosz, "Motif-based design for connected vehicle systems in presence of heterogeneous connectivity structures and time delays," *IEEE Transactions on Intelligent Transportation Systems*, vol. 17, no. 6, pp. 1638–1651, 2016.

[6] J. I. Ge, S. S. Avedisov, C. R. He, W. B. Qin, M. Sadeghpour, and G. Orosz, "Experimental validation of connected automated vehicle design among human-driven vehicles," *Transportation Research Part C*, vol. 91, pp. 335–352, 2018.

[7] C. R. He, H. Maurer, and G. Orosz, "Fuel consumption optimization of heavy-duty vehicles with grade, wind, and traffic information," *Journal of Computational and Nonlinear Dynamics*, vol. 11, no. 6, p. 061011, 2016.

[8] Navistar, "Maxxforce 11 and 13 liter engines," Navistar Inc., Tech. Rep., 2011.

[9] N. I. Li, C. R. He, and G. Orosz, "Sequential parametric optimization for connected cruise control with application to fuel economy optimization," in *Proceedings of the 55th IEEE Conference on Decision and Control*, 2016, pp. 227–232.

A APPROXIMATING THE ENERGY CONSUMPTION

In this Appendix we provide the detailed derivation of the cost function (22).

Recall the truck's speed response (20) for a certain parameter set $\mathbf{p}_n$, we have

$$\begin{aligned} v(t) &= v^* + \tilde{v}(t) \\ &= v^* + \sum_{j=1}^{m} D_j \sin(\omega_j t + \theta_j)\,, \end{aligned} \tag{23}$$

where $t \in [0, T]$, $\omega_j = j\Delta\omega$, $j = 1, \ldots, m$, and $\Delta\omega = 2\pi/T$. Correspondingly, the acceleration of the truck is

$$\dot{v}(t) = \sum_{j=1}^{m} D_j \omega_j \cos(\omega_j t + \theta_j)\,. \tag{24}$$

Note that the nonlinear function $g(x) = \max(x, 0)$ in (9) can be approximated by

$$\hat{g}(x) = \frac{1}{2}\left(x + \frac{x^2}{\sqrt{\varepsilon + x^2}}\right), \tag{25}$$

for small $\varepsilon > 0$.

To approximate the total energy consumption we omit $f(v)$ in (9), that is,

$$\hat{w} = \int_0^T v\,\hat{g}\big(\dot{v}\big)\,\mathrm{d}t = \frac{1}{2}\int_0^T \frac{v\,\dot{v}^2}{\sqrt{\varepsilon + \dot{v}^2}}\,\mathrm{d}t\,. \tag{26}$$

Note that

$$\dot{v}^2 = \sum_{j,k=1}^{m} D_j D_k \omega_j \omega_k \cos(\omega_j t + \theta_j)\cos(\omega_k t + \theta_k)\,. \tag{27}$$

Thus, for some $M > 0$, we have

$$\varepsilon \le \varepsilon + \dot{v}^2 \le \varepsilon + \sum_{j,k=1}^{m} D_j \omega_j D_k \omega_k \le M \sum_{j=1}^{m} D_j^2 \omega_j^2\,, \tag{28}$$

where in the last step we utilized the Cauchy-Schwarz inequality. Thus, we obtain the bounds

$$\frac{\displaystyle\int_0^T v\,\dot{v}^2 \mathrm{d}t}{2\sqrt{M \displaystyle\sum_{j=1}^{m} D_j^2 \omega_j^2}} \le \hat{w} \le \frac{\displaystyle\int_0^T v\,\dot{v}^2 \mathrm{d}t}{2\sqrt{\varepsilon}}\,. \tag{29}$$

On the other hand,

$$\begin{aligned} v^*\dot{v}^2 = \frac{v^*}{2}\sum_{j=1}^{m} D_j^2\omega_j^2 - \frac{v^*}{2}\sum_{j=1}^{m} D_j^2\omega_j^2 \cos(2\omega_j t + 2\theta_j) \\ + \frac{v^*}{2}\sum_{j=1}^{m}\sum_{k=1,k\neq j}^{m} D_j D_k \omega_j \omega_k \\ \times \Big[\cos\big((\omega_j + \omega_k)t + \theta_j + \theta_k\big) \\ + \cos\big((\omega_j - \omega_k)t + \theta_j - \theta_k\big)\Big], \end{aligned} \tag{30}$$

and

$$\begin{aligned}\tilde{v}\,\dot{v}^2 &= \sum_{j=1}^{m}\sum_{k=1}^{m}\sum_{l=1}^{m} D_j D_k D_l \omega_j \omega_k \\ &\quad \times \cos(\omega_j t+\theta_j)\cos(\omega_k t+\theta_k)\sin(\omega_l t+\theta_l) \\ &= \frac{1}{4}\sum_{j=1}^{m}\sum_{k=1}^{m}\sum_{l=1}^{m} D_j D_k D_l \omega_j \omega_k \\ &\quad \times \Big[\sin\big((\omega_j+\omega_k+\omega_l)t+\theta_j+\theta_k+\theta_l\big) \\ &\quad -\sin\big((\omega_j+\omega_k-\omega_l)t+\theta_j+\theta_k-\theta_l\big) \\ &\quad +\sin\big((\omega_j-\omega_k+\omega_l)t+\theta_j-\theta_k+\theta_l\big) \\ &\quad -\sin\big((\omega_j-\omega_k-\omega_l)t+\theta_j-\theta_k-\theta_l\big)\Big]. \end{aligned} \tag{31}$$

Thus, adding (30) and (31) and evaluating the integrals, we obtain

$$\begin{aligned}\int_0^T v\,\dot{v}^2 \mathrm{d}t &= \frac{T}{2}v^*\sum_{j=1}^{m} D_j^2\omega_j^2 \\ &+ \frac{T}{4}\sum_{j=1}^{m-1}\sum_{k\le m-j}^{m} D_j D_k D_{j+k}\omega_j\omega_k \sin(\theta_{j+k}-\theta_j-\theta_k) \\ &+ \frac{T}{2}\sum_{j=1}^{m-1}\sum_{k>j}^{m} D_j D_k D_{k-j}\omega_j\omega_k \sin(\theta_j+\theta_{k-j}-\theta_k).\end{aligned} \tag{32}$$

Here, we assume the speed oscillations are small compared to the steady-state speed, that is, $v^* \gg D_j$ for $j=1,\dots,m$. Then denoting $\overline{D}=\max\{D_j|j=1,\dots,m\}$. Thus, we have

$$\begin{aligned}&\Big|\sum_{j=1}^{m-1}\sum_{k\le m-j}^{m} D_j D_k D_{j+k}\omega_j\omega_k \sin(\theta_{j+k}-\theta_j-\theta_k)\Big| \\ &\le \sum_{j=1}^{m-1}\sum_{k\le m-j}^{m} D_j D_k D_{j+k}\omega_j\omega_k < m\overline{D}\sum_{j=1}^{m}\omega_j^2 D_j^2,\end{aligned} \tag{33}$$

and

$$\begin{aligned}&\Big|\sum_{j=1}^{m-1}\sum_{k>j}^{m} D_j D_k D_{k-j}\omega_j\omega_k \sin(\theta_j+\theta_{k-j}-\theta_k)\Big| \\ &\le \sum_{j=1}^{m-1}\sum_{k>j}^{m} D_j D_k D_{k-j}\omega_j\omega_k < \frac{m\overline{D}}{2}\sum_{j=1}^{m}\omega_j^2 D_j^2,\end{aligned} \tag{34}$$

yielding

$$\begin{aligned}&\frac{(v^*-m\overline{D})T}{2}\sum_{j=1}^{m} D_j^2\omega_j^2 \\ &\le \int_0^T v\,\dot{v}^2\mathrm{d}t \le \\ &\frac{(v^*+m\overline{D})T}{2}\sum_{j=1}^{m} D_j^2\omega_j^2.\end{aligned} \tag{35}$$

Finally, the energy consumption (26) can be bounded as

$$\underline{C}\sqrt{\sum_{j=1}^{m} D_j^2\omega_j^2} \le \hat{w} \le \overline{C}\sum_{j=1}^{m} D_j^2\omega_j^2, \tag{36}$$

where

$$\underline{C}=\frac{(v^*-m\overline{D})T}{4\sqrt{M}}, \quad \overline{C}=\frac{(v^*+m\overline{D})T}{4\sqrt{\varepsilon}}. \tag{37}$$

Given $v^* > m\overline{D}$, the energy consumption (26) is bounded by class-$\mathcal{K}$ functions of $\sqrt{\sum_{j=1}^{m} D_j^2\omega_j^2}$, which can be used for a robust energy-optimal design; see (22).